Suppression of the soliton self-frequency shift and compression in the presence of bandwidth-limited amplification

Ivan M. Uzunov* and Todor N. Arabadzhiev
Department of Applied Physics, Technical University – Sofia, 8 Kl. Ohridski Blvd., Sofia 1000, Bulgaria
(Received 21 December 2010; revised manuscript received 30 May 2011; published 9 August 2011)

We study numerically the suppression of the soliton self-frequency shift as well as the compression in the presence of bandwidth-limited optical amplification (BLA). Our results confirm the existence of equilibrium points (stable focuses) for the soliton amplitude and speed identified by the soliton perturbation theory. Analyzing the equilibrium amplitudes as a function of physical parameters, maximum compression factor in the amplification of short pulses is revealed. The results of linear stability analysis allow estimation of the necessary distance for the appearance of equilibrium states from different initial conditions. It has been shown that the shape of the perturbed stationary solution in the presence of intrapulse Raman scattering and BLA can be described by the earlier derived analytic expressions.

DOI: 10.1103/PhysRevE.84.026607 PACS number(s): 05.45.Yv

I. INTRODUCTION

As is well known, the intrapulse Raman scattering (IRS) is related to the delayed nature of the Raman response in optical fibers and plays an important role in the propagation of femtosecond optical pulses [1–6]. The first demonstration of the Raman soliton self-scattering effect was presented in [7]. High-frequency components of femtosecond optical pulses can transfer energy to its low-frequency components, which results in downshift of the soliton carrier frequency, a phenomenon known as the soliton self-frequency shift (SSFS) [8]. The broadband soliton supercontinuum due to the decay of higher-order solitons (the Satsuma-Yajima N-soliton bound state) was established in [9–11]. Numerical Zakharov-Shabat eigenvalue analysis of this effect has been presented in [12]. Recently, the decay of higher-order solitons is one of the basic mechanisms for obtaining supercontinuum spectral broadening in microstructured optical fibers [13–15]. Propagating fundamental solitons with high amplitude ($\eta = 10$) in the presence of IRS leads to soliton compression [3]. An important difference with soliton-effect compressors, where during compression a broad pedestal appears, is that due to the SSFS the compressed soliton separates from the pedestal. As a result, a redshifted and pedestal-free pulse with a compression factor larger than in the standard soliton-effect compressors appears [3]. Adiabatic approximations of perturbation theory (PT) for the description of parameters of bright and dark solitons in the presence of IRS have been proposed in [16] and [17], respectively. The full perturbation theory, which includes not only the change of the soliton parameters, but also the changes in the shape of the bright solitons, has been developed in [10] and [18]. Group theory analysis of IRS of bright solitons in single mode fibers and strongly birefringent fibers has been proposed in [19] and [20], respectively. Recently, it was shown that IRS can be approximately described by the nonlinear Schrödinger equation with a linear external potential [21–23], known as the Chen and Liu model, in linearly inhomogeneous plasma [24]. The circumstance that the Chen and Liu model is integrable by means of the inverse scattering method has been used to explain the stability of the solitons in the presence of IRS [21–23].

One possibility to suppress the IRS provides third-order dispersion [25,26]. As is well known, third-order dispersion (TOD) (provided the corresponding coefficient is positive) forms a peak in the blue spectral region at a frequency which is inversely proportional to the strength of TOD. If the resonance peak is located within the Raman gain band, the IRS-induced redshift of the single soliton spectrum can be partially suppressed [25,26]. Moreover, because of IRS the resonance radiation is eventually transferred back to the spectral region around the carrier frequency [27]. The interplay between TOD and IRS was studied with a numerical Zakharov-Shabat eigenvalue analysis in [12].

It was also shown that the SSFS can be reduced using optical fibers with spectrally inhomogeneous frequency dependence of the group-velocity dispersion [21,22,28,29]. The passage of a femtosecond soliton through a potential barrierlike spectral inhomogeneity of group-velocity dispersion, including the forbidden band of positive group-velocity dispersion [29], has been established. This effect has been called the soliton spectral tunneling effect [21,22,29]. Sufficient increase of the height of the spectral barrier leads to the full suppression of SSFS [22].

Because of their large bandwidth, erbium-doped fiber amplifiers (EDFAs) can be used to amplify optical pulses in fiber lasers and long-haul fiber-optic communication systems [1–6,30]. In the case of adiabatic amplification ($\delta < 1$, see below) the amplified fundamental soliton with $\eta = 1$ adjusts its parameters, so the initial soliton pulse is compressed. Simultaneously, however, subpulses are generated and their numbers increase with propagation distance [3,30]. When relatively short (about 1 ps) pulses have to be amplified, IRS should also be taken into account. It was established [31–33] that the bandwidth-limited optical amplification (BLA) with the gain dispersion taken in the parabolic approximation (see below) can reduce the amount of spectral shift due to the SSFS and stabilize the carrier frequency of the fundamental soliton with $\eta = 1$ close to the gain peak, phenomena known as suppression of the SSFS by BLA [31]. The amplification and compression of short pulses in the presence of IRS have been numerically studied by different physical models in [33],

*ivan_uzunov@tu-sofia.bg

where the compression factor and the parameters of subpulses were studied. The adiabatic approximation of PT has been employed in the study of the suppression of the SSFS by BLA and the equilibrium point for the soliton amplitude and speed has been identified in [31,33–35]. The relation between the equilibrium speed and the amplitude of the perturbed soliton was found [31,33–35]. An analytical solution for the eigenvalues of the linearized problem in the vicinity of the equilibrium point is proposed in [35]. A perturbation approach for analysis of the same problem has been proposed that uses the equation of the strongly nonlinear Duffing–Van der Pol oscillator [35]. This approach is based on the usage of hyperbolic perturbation methods of [36,37]. The equilibrium velocity as well as its coupling to the amplitude of the perturbed stationary solution have been found [35]. It turned out that this coupling is similar to the relation between the soliton amplitude and speed derived by the adiabatic approximation of PT [31,33–35]. Applying [37], the form of the perturbed stationary solution has been evaluated [35] and it was found to be similar to the one found earlier in [10,18,19].

The aim of this paper is to numerically study the suppression of the SSFS as well as the compression of short pulses in the presence of BLA. BLA is studied in the parabolic approximation. Using the eigenvalues of the linearized problem [35], the type of equilibrium points will be identified. Analyzing the equilibrium amplitudes as a function of physical parameters, the maximum compression factor in the amplification of short pulses will be studied. It will be shown that the eigenvalues of the linearized problem allow estimation of the necessary distance of propagation for the appearance of equilibrium states from different initial conditions. Special attention will be paid to the equilibrium fundamental solitons with large amplitudes. All results obtained by perturbation theory will be verified by numerical solution of the basic equation. Finally, changes in the shape of the perturbed soliton in the presence of BLA and IRS will be numerically explored and the results compared with earlier analytical predictions [10,18,19,35].

II. BASIC EQUATION AND PERTURBATION RESULTS

The erbium ions in doped fiber can be modeled as a two-level system. The Maxwell-Bloch equations for the slowly varying part of the polarization, responsible for the contribution of dopant and the population inversion density, together with the modified nonlinear Schrödinger equation (NLSE) for the slowly varying envelope of the electric field should be solved together [3,30]. Considering optical pulses with widths larger than that of the dipole relaxation time $T_2 \approx 0{,}1$ ps, the rate-equation approximation in which the polarization follows the optical field adiabatically can be used. The dispersive effects connected with the erbium ions can be included through the dopant susceptibility into the refractive index change and then into the modified NLSE. The important sequence of this procedure is that the dispersion parameters of the fiber become dependent on the dopant content [3]. It turned out that the dopant-induced change in the group velocity is negligible in practice, while the additional term to the group-velocity dispersion should be taken into account. This additional term represents the finite bandwidth of the fiber amplifier and is referred to as gain dispersion (see below). If the mode density and the dopant density are nearly uniform over the doped region and zero outside it, the relationship between the small-signal gain and the population inversion density transforms to a linear one. In general, the dynamics of the gain depends on the small-signal gain, the fluorescence time (10 ms for EDFA), the saturation energy, and the pumping configuration. For short optical pulses, the dependence on the pumping configuration is neglected [3]. As the typical pulse energy is much smaller than the saturation energy of EDFA (1 μJ), the gain saturation can be neglected. Finally, the following modified NLSE describes the pulse amplification in erbium-doped single mode optical fiber [1–4]:

$$i\frac{\partial U}{\partial x} + \frac{1}{2}\frac{\partial^2 U}{\partial t^2} + |U|^2 U = i\delta U + i\beta\frac{\partial^2 U}{\partial t^2} + \gamma U\frac{\partial}{\partial t}(|U|^2), \tag{1}$$

where the dimensionless variables (soliton units) are introduced as follows [3]:

$$x = z/L_D, \quad t = T/T_0, \quad U = (\gamma L_D)^{1/2} A.$$

Here, z and t' are real longitudinal coordinates in the fiber and time, $T = t' - z/v_g = t' - \beta_1 z$, v_g is the group velocity, $A(z,T)$ is the slowly varying envelope, $L_D = T_0^2/|\beta_2|$ is the dispersion length, T_0 is the width of the pulse, and β_2 represents the dispersion of the group velocity. $\gamma = n_2\omega_0/cA_{\text{eff}}$ is the nonlinear parameter, n_2 is the nonlinear-index coefficient, ω_0 is the carrier wavelength of the optical pulse, A_{eff} is the effective core area, and c is the speed of light in vacuum. Next,

$$\delta = (g_0 - \alpha)L_D/2, \quad \beta = g_0 L_D (T_2/T_0)^2/2,$$

where g_0 is the peak (small-signal) gain and α is the fiber losses [3]. The term proportional to β represents the finite bandwidth of the amplifier. In Eq. (1) it is assumed that the detuning parameter is zero as well as that the pulse spectrum is narrower than the gain bandwidth (parabolic approximation for the gain) [3,30]. Numerical values of the parameters δ, β for most EDFAs and pulse width $T_0 \approx 1$ ps are $\delta \approx 0.5$ and $\beta \approx 0.5 \times 10^{-3}$ [3]. The last term on the left-hand side of Eq. (1) is proportional to $\gamma = T_R/T_0$, where $T_R (\approx 3$ fs at $\lambda \approx 1.55$ μm) is related to the first moment of the nonlinear response function (the slope of the Raman gain spectrum) [3]. This term is related to the delayed Raman response, describes the IRS, and is consequently responsible for the SSFS. Analyzing the breakup of higher-order solitons in the presence of IRS, the splitting of the real parts of the eigenvalues related to the soliton solutions at $\gamma = 10^{-4} (T_0 \approx 30$ ps) and the change of the imaginary parts at $\gamma = 5 \times 10^{-3} (T_0 \approx 600$ fs) have been established [12]. If the pulse width is close to T_R, the more general model for description of the amplification of femtosecond optical pulses should be used [3,21,30,33,38,39].

If the Raman term in Eq. (1) is neglected, the resultant equation has exact chirped solutions [4]. To the best of our knowledge, Eq. (1) has no exact solutions. In accordance with PT for a small δ, β, γ, the soliton solution of Eq. (1) may be written as [1,18]

$$U(x,t) = \eta(x)\text{sech}\{\eta(x)[t - \tau(x)]\}\exp\{i[-k(x)t + \sigma(x)]\}, \tag{2}$$

where $\eta(x)$ and $k(x)$ are the soliton amplitude and speed (frequency), respectively. The speed $k(x)$ represents the derivation from the group velocity as well as the frequency shift. The soliton position $\tau(x)$ and phase $\sigma(x)$ are defined by the equations $d\tau(x)/dx = -k$ and $d\sigma(x)/dx = (\eta^2 - k^2)/2$, respectively. The relation between $k(x)$ and the change of the group velocity is as follows: $\Delta v_g = (v_g^2|\beta_2|k)/T_0$, so for $k < 0$, the soliton moves at a speed lower than the group velocity and $\Delta v_g < 0$. Applying PT, the following system of ordinary differential equations that describe the evolution of amplitude and speed can be derived [1,18,33,34]:

$$\frac{d}{dx}\eta = 2\delta\eta - 2\beta\left(k^2 + \frac{1}{3}\eta^2\right)\eta, \quad \frac{d}{dx}k = -\frac{4}{3}\beta k\eta^2 - \frac{8}{15}\gamma\eta^4. \tag{3}$$

The following equilibrium point (EP) has been identified [31,33–35]:

$$\eta_{\rm PT} = \sqrt{\frac{(5\sqrt{25\beta^4 + 144\delta\beta\gamma^2} - 25\beta^2)}{24\gamma^2}}, \qquad k_{\rm PT} = -\frac{(\sqrt{25\beta^4 + 144\delta\beta\gamma^2} - 5\beta^2)}{12\beta\gamma}. \tag{4}$$

The equilibrium values of speed $k_{\rm PT}$ and the square of amplitude $\eta_{\rm PT}^2$ are related by the equation [30,33–35]

$$k_{\rm PT} = -2\gamma\eta_{\rm PT}^2/(5\beta). \tag{5}$$

The physical meaning of the soliton with the equilibrium values of amplitude and frequency given by Eq. (4) is as follows: During the process of the adiabatic amplification, the initial soliton compresses, and due to the SSFS, at some point it escapes from the amplifier bandwidth. As a result, the amplification process stops and soliton amplitude and frequency stabilize to their stationary values given by the EP. The analytical solution for the eigenvalues $\lambda_{1,2}$ of the linearized problem in the vicinity of the EP is [35]

$$\lambda_{1,2} = (-p \pm \sqrt{p^2 - 4q})/2, \tag{6}$$

where the quantities q, p, and Λ are defined by $p = 5\beta(-5\beta^2 + \sqrt{25\beta^4 + 144\delta\beta\gamma^2})/(9\gamma^2)$, $q = 5\beta(-125\beta^5 - 720\gamma^2\beta^2\delta + (25\beta^3 + 72\gamma^2\delta)\sqrt{\Lambda})/(162\gamma^4)$, and $\Lambda = 25\beta^4 + 144\beta\gamma^2\delta$. In our region of values of parameters (see below) $q > 0$ (and $p > 0$), therefore the EP given by Eq. (4) is a simple one. For $p^2 < 4q$, the roots λ_1 and λ_2 are complex conjugate and the stable focal points appear. This is the general case studied in this paper. In the degenerate root case $p^2 = 4q$, the roots $\lambda_1 = \lambda_2 = -p/2$ are degenerate and a nodal point is obtained. We will further study a situation very similar to this one. (Note that when $\delta < 0$, $\beta > 0$, and $\gamma > 0$, then $q > 0$, $p^2 - 4q > 0$, and $p < 0$, the EP is an unstable nodal point.) For $\gamma = 0$, the system (3) has an equilibrium point with zero amplitude, which in the case of $\delta > 0$ and frequency $k_0^2 < \delta/\beta$ is unstable. As a sequence, small amplitude (dispersive) waves grow exponentially, or background instability appears.

Perturbation approach for the analysis of the stationary solution of Eq. (1) based on the ansatz

$$U(x,t) = u(\xi)\exp\{i\,[f\,(\xi) + Kx]\}, \tag{7}$$

where $\xi = t - Mx$ (M and K are real numbers) was proposed in [35]. The equation of the strongly nonlinear Duffing–Van der

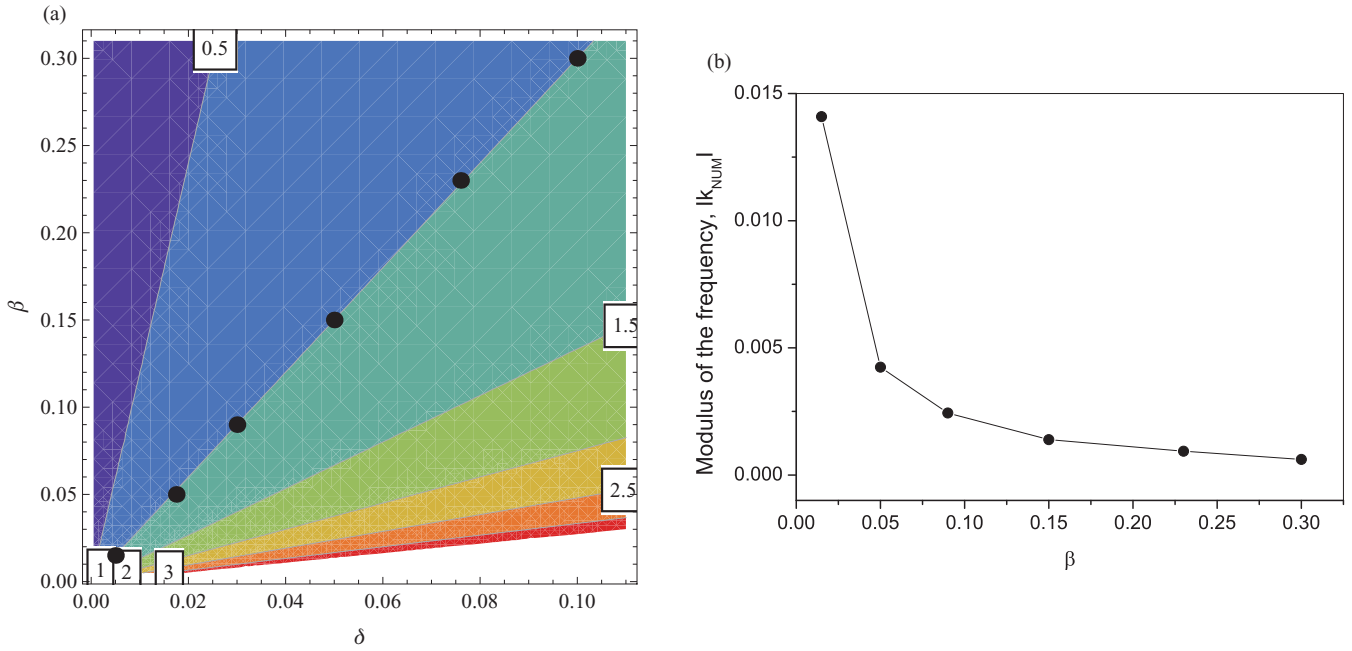

FIG. 1. (Color online) (a) The contoured plots present dependence $\eta_{\rm PT} = \eta_{\rm PT}(\delta,\beta)$ for $\gamma = 5 \times 10^{-4}$ and the white squares present the value of the equilibrium amplitude in each area. The black points mark values of δ and β for which the appearance of the ES was numerically studied. (b) The dependence of $|k_{\rm num}|$ of the ES as a function of β ($\delta \sim \beta/3$), $\gamma = 5 \times 10^{-4}$.

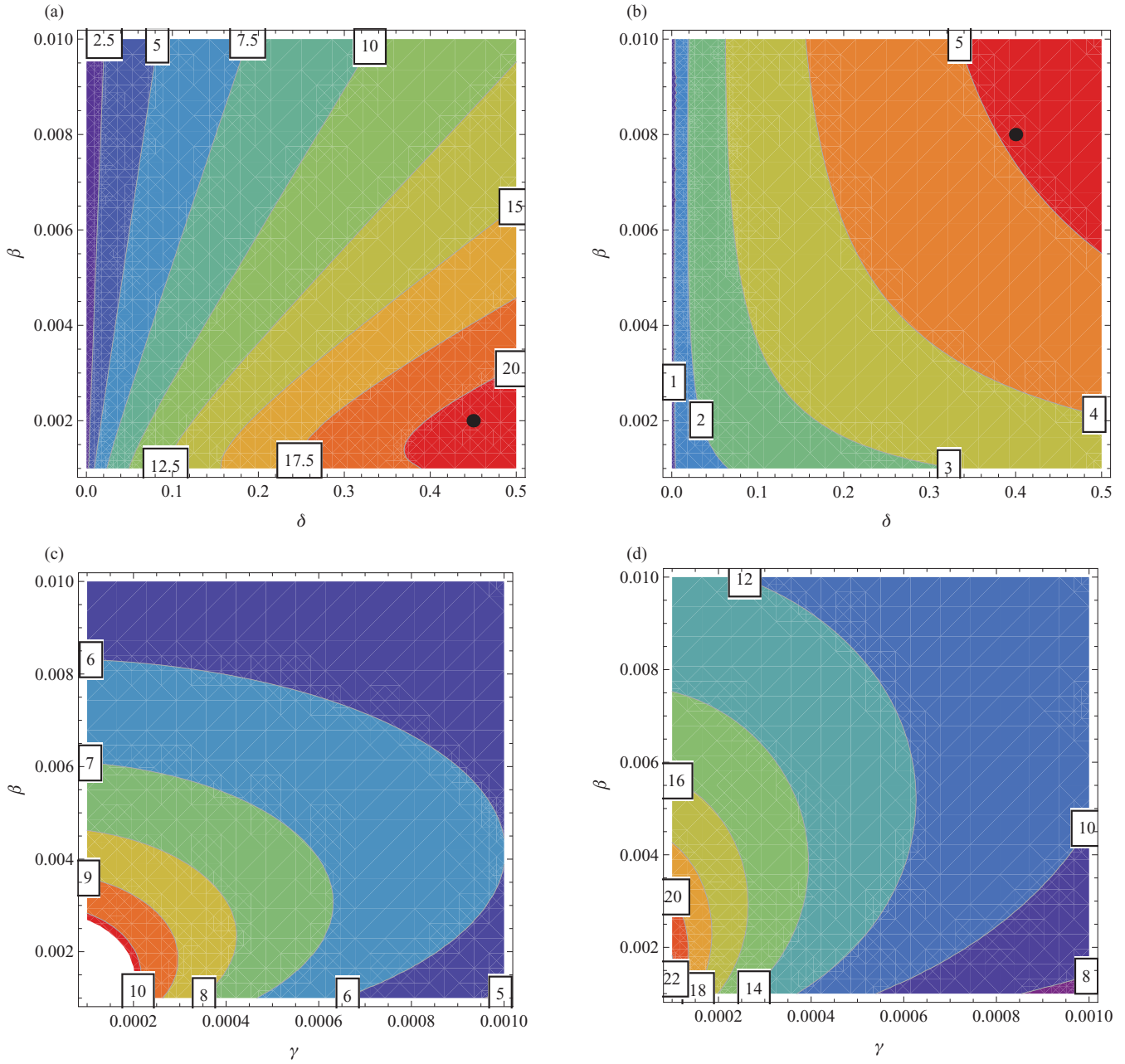

FIG. 2. (Color online) The contoured plots present $\eta_{PT} = \eta_{PT}(\delta,\beta)$ for (a) $\gamma = 10^{-4}$ and (b) $\gamma = 5 \times 10^{-3}$, and $\eta_{PT} = \eta_{PT}(\gamma,\beta)$ for $\delta = 0.1$ (c) and $\delta = 0.5$ (d). [Points in (a) and (b) are explained in text.]

Pol oscillator was introduced for the approximate description of the function $u(\xi)$ [35]:

$$u'' + c_1 u + c_3 u^3 = \varepsilon(\mu - \mu_1 u^2)u', \tag{8}$$

where $c_1 = -2K$, $c_3 = 2$, $\mu = -4\beta M/\gamma$, and $\mu_1 = -4$. μ is a control parameter in the methods [36,37]. The critical values μ_{C0} and M_{C0}, for the formation of the perturbed solution of Eq. (8), were found [35]:

$$M_{C0} = 2\gamma a_0^2/(5\beta), \tag{9}$$

where $a_0^2 = -2c_1/c_3 = 2K$. Similarity between Eqs. (6) and (9) was mentioned [35]. The perturbed solution of Eq. (8) was found by means of [37] in [35]:

$$u(\omega_0\xi) = a_0\{1 - (4\gamma a_0/5)\ln[\cosh(\omega_0\xi)]\tanh(\omega_0\xi)\}\mathrm{sech}(\omega_0\xi), \tag{10}$$

where $\omega_0^2 = -c_1 = 2K$.

III. COMPARISON OF ANALYTICAL AND NUMERICAL RESULTS

To verify the properties of the equilibrium solitons (ES) obtained by PT, we numerically solve Eq. (1) for the following values of parameters: $\delta \subset (5 \times 10^{-3}, 0.5)$,

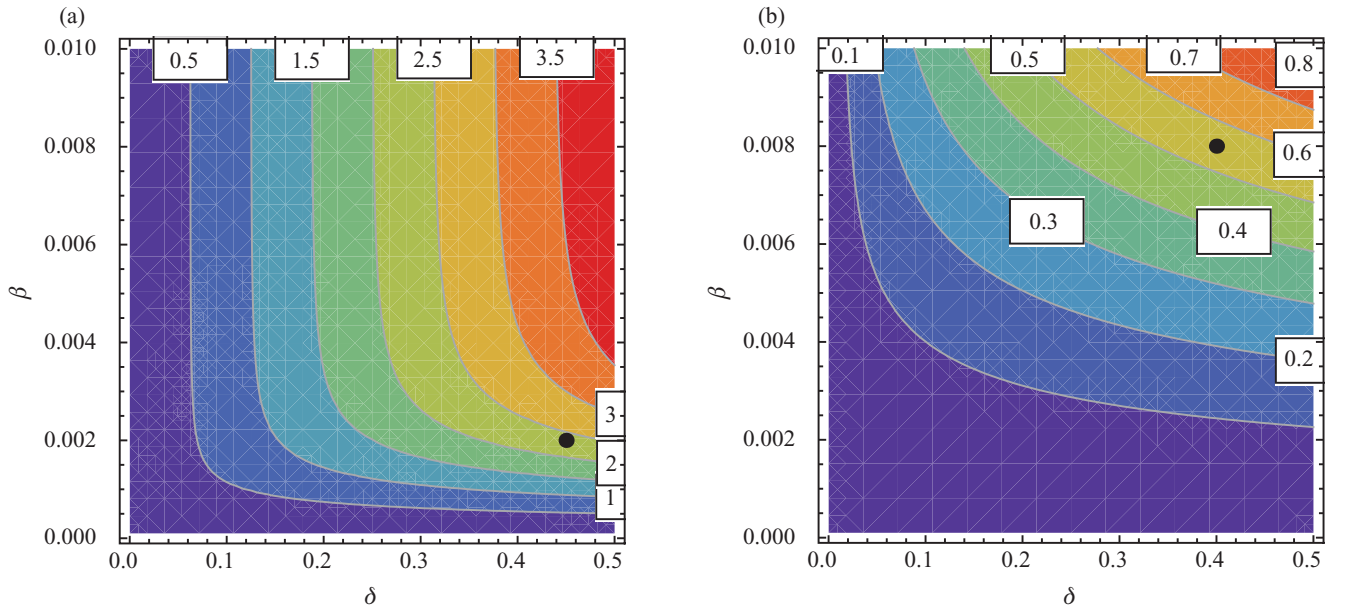

FIG. 3. (Color online) The contoured plots of $p(\delta,\beta)$ as a function of δ and β for (a)$\gamma = 10^{-4}$ and (b) $\gamma = 5 \times 10^{-3}$. [Points in (a) and (b) are explained in text.]

$\beta \subset (1 \times 10^{-3}, 0.3)$, and $\gamma \subset (10^{-4}, 0.3)$. As $\delta > 0$, background instability appears. For numerical investigation of Eq. (1), the scheme of the split-step Fourier method proposed in [38] was applied. To check the correctness of the Blow-Wood RK4 scheme, the error of the evolution of the two-soliton bound state in the presence of IRS was calculated and good agreement with the results of [40] was established. The evolution of the amplitude and frequency of solitons with distance was calculated, identifying their equilibrium values η_N and k_N. The time evolution of the amplitude's maximum of the pulse with distance x, or $dt/dx = 1/c$, was studied. The velocity c here characterizes the time shift of the soliton and it is related to the change of its group velocity: $\Delta v_g = -(v_g^2|\beta_2|)/(cT_0)$. If $c > 0$, the soliton moves at a speed lower than the group velocity and $\Delta v_g < 0$. Then, $k_N = -1/c$. To compare the numerical (η_N and k_N) and analytical ($\eta_{\rm PT}$ and $k_{\rm PT}$) parameters of equilibrium solitons, the errors $\Delta\eta = |\eta_N - \eta_{\rm PT}|/\eta_N$ and $\Delta k = |k_N - k_{\rm PT}|/|k_N|$ are used.

Using the eigenvalues of the linearized problem in the vicinity of the EP [Eq. (6)], it was shown that in the region of discussed values of parameters, $p^2 < 4q$, so the EPs are stable focuses. To obtain the EP by numerical solution of Eq. (1) or Eq. (3) starting with different initial conditions, a certain minimum distance of propagation $x_{\rm EP}$ is required. The EP given by Eq. (4) can be used for two purposes. First, they can be used to obtain required parameter values for which the initial fundamental soliton, with $\eta = 1$, reduces its SSFS. Second, as we will see, the EP gives the parameters of ES that appear as a result of pulse compression of initial fundamental solitons, with $\eta = 1$ due to the BLA. In the second case the question arises, which are the maximum values of soliton amplitudes and therefore the maximum factor of compression?

Our first aim is to verify the description of suppression of SSFS for the fundamental soliton $\eta = 1$. We should mention that solving Eq. (3), two ES related to the stable focus were reported earlier: (a) equilibrium parameters $\eta_{\rm PT} = 0.99$, $k_{\rm PT} = -0.35$, $x_{\rm EP} \sim 80$ for the case of $\delta = 2.5 \times 10^{-2}$, $\beta = 5.6 \times 10^{-2}$, and $\gamma = 5 \times 10^{-2}$ [18], respectively, and (b) equilibrium parameters $\eta_{\rm PT} = 2.3$, $k_{\rm PT} = -2.12$, and $x_{\rm EP} \sim 60$ for $\delta = 0.25$, $\beta = 4 \times 10^{-2}$, and $\gamma = 4 \times 10^{-2}$ [30]. In both cases the observed values of $x_{\rm EP}$ are large.

We examined the dependence of $\eta_{\rm PT}$ on the δ,β for $\gamma = 5 \times 10^{-4}$. δ and β satisfy the relation $\delta \sim \beta/3$ as for the case of BLA ($\gamma = 0$) [1,41,42]. It was not possible to analytically find the maximum of $\eta_{\rm PT}$ as a function of δ, β, and γ, so we numerically plot $\eta_{\rm PT} = \eta_{\rm PT}(\delta,\beta)$ for $\gamma = 5 \times 10^{-4}$ in Fig. 1(a). We took the parameter values [as shown in Fig. 1(a)], so the amplitudes of ES equal to 1 were expected. Next we numerically solve Eq. (1) for the chosen parameters, and ES were observed with parameters shown in Fig. 1(b).

Figure 1(b) illustrates the suppression of the SSFS: with the increase of β, the modulus of the equilibrium velocities $|k_N|$ reduces. As anticipated, the amplitudes of ES η_N tend to unity. In this case $p^2 \sim 4q$ (with accuracy of 10^{-6}), so the EP can be considered as a "nodes," $10 \leqslant x_{\rm EP} \leqslant 70$. The maximum values of errors are of the order of several percent for amplitudes and twice larger for the frequency. One reason for frequency errors is the small values of frequencies that make their calculation difficult. For small equilibrium amplitudes the background instability waves observed in simulations are small. The appearance of EPs has been confirmed using different initial conditions $U(0,t) = \eta\,\mathrm{sech}(\eta t)$, $\eta \subset (2,20)$.

Our second aim is to find the maximum values of soliton amplitudes, and therefore the maximum factor of compression of initial fundamental solitons, with $\eta = 1$ due to the BLA. We numerically plot two types of dependences: (a) $\eta_{\rm PT} = \eta_{\rm PT}(\delta,\beta)$ for two different values of $\gamma = 1 \times 10^{-4}$ and $\gamma = 5 \times 10^{-3}$ [Figs. 2(a) and 2(b)], and (b) $\eta_{\rm PT} = \eta_{\rm PT}(\gamma,\beta)$ for two different values of $\delta = 0.1$ and $\delta = 0.5$ [Figs. 2(c) and 2(d)].

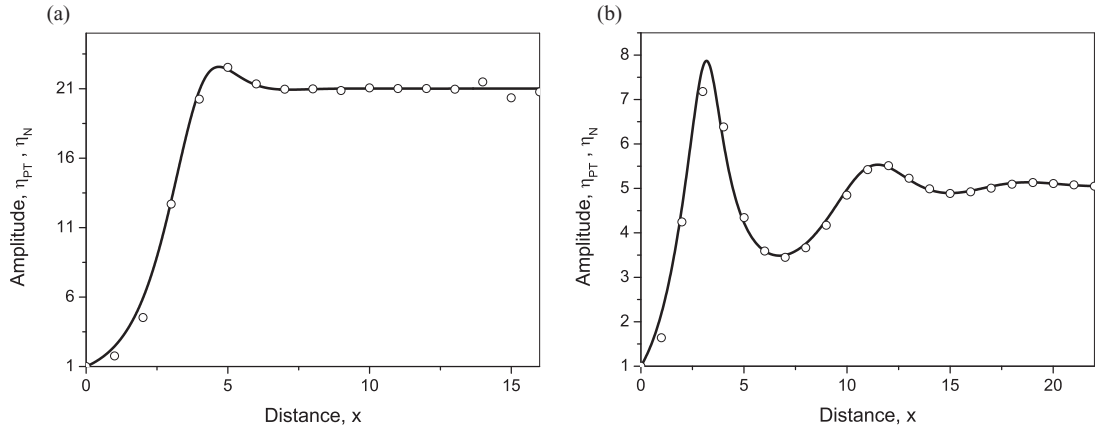

FIG. 4. Evolution of pulse amplitude with distance according to Eq. (3) (solid line) and the numerical solution of Eq. (1) (empty circles) for (a) $\delta = 0.45$, $\beta = 2 \times 10^{-3}$, and $\gamma = 10^{-4}$ and (b) $\delta = 0.4$, $\beta = 8 \times 10^{-3}$, and $\gamma = 5 \times 10^{-3}$, respectively.

Figure 2(a) reveals a very well expressed region in the parametric space of parameters δ and β where the maximum values of η_{PT} of an order of 20 can be obtained. Figure 2(b) shows, however, that with the increase of γ, the maximum values of η_{PT} reduce sensitively, and in addition, the region is shifted in the direction of larger β. So we can expect that there is a proper initial pulse width T_0 for which the maximum compression is possible. Figures 2(c) and 2(d) show the influence of the gain δ for increasing the maximum values of η_{PT}. With the increase of the value of δ, the maximum values of η_{PT} increase from 10 in Fig. 2(c) to 22 in Fig. 2(d). In this case the region of maximum values does not change with the change of δ. Keeping in mind that increasing the gain of EDFAs δ can be larger than 1 (for EDFA providing a 10 dB gain over L_D, δ is of the order of 1) we can expect even larger maximum values of η_{PT}.

The eigenvalues $\lambda_{1,2}$ of the linearized problem in the vicinity of the EP allow the determination of the type of the EP. The magnitude of p [see Eq. (6)] determines the minimum distance of propagation x_{EP} for which the initial fundamental soliton with $\eta = 1$ compresses and achieves its equilibrium parameters. In Fig. 3 we plot $p(\delta,\beta)$ as a function of δ, and β for two values of γ for $\gamma = 10^{-4}$ [Fig. 3(a)] and $\gamma = 5 \times 10^{-3}$ [Fig. 3(b)], respectively.

As can be seen from Figs. 3(a) and 3(b) for fixed γ, p increases with δ and β. With an increase of γ for fixed values of δ and β, p is reduced. To obtain the certain value of compression factor for the minimum x_{EP}, we first should choose the proper values of the parameters δ, β, and γ from Fig. 2. Next, from Fig. 3 we should choose the maximum possible value of p, which will provide the minimum x_{EP}. Such an example is presented in Fig. 4. In Figs. 4(a) and 4(b) we compare the results for amplitude obtained by numerical solution of Eqs. (1) and (3) (initial condition $\eta = 1$, $k = 0$) for the cases (a) $\delta = 0.45$, $\beta = 2 \times 10^{-3}$, and $\gamma = 10^{-4}$ and (b) $\delta = 0.4$, $\beta = 8 \times 10^{-3}$, and $\gamma = 5 \times 10^{-3}$, respectively. The expected equilibrium amplitudes (therefore the compression factors) and values of p are presented by points in Figs. 2(a) and 3(a) and Figs. 2(b) and 3(b), respectively. According to Eq. (4) the equilibrium values of soliton parameters are $\eta_{PT} = 21.007$ and $k_{PT} = -8.826$ for the first case [Fig. 2(a)], and $\eta_{PT} = 5.074$ and $k_{PT} = -6.436$ for the second case [Fig. 2(b)]. Using Eq. (6) the following values

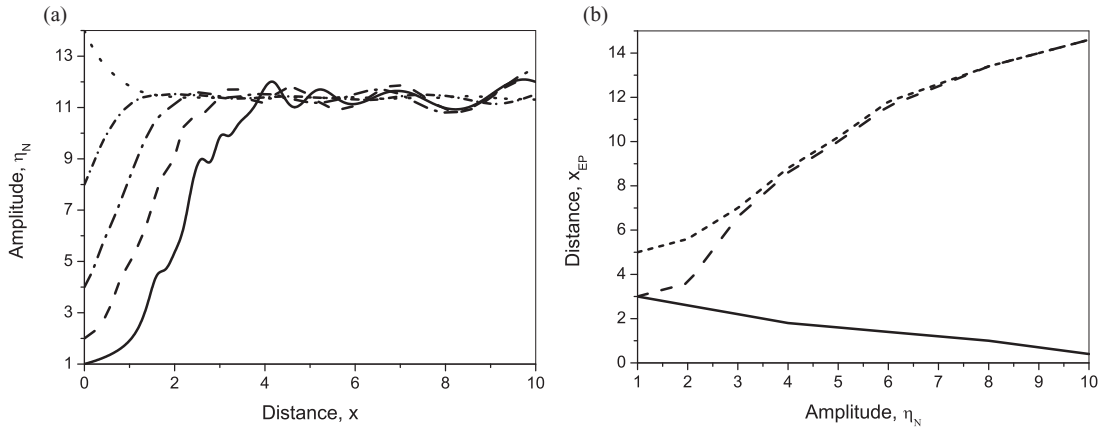

FIG. 5. (a) Peak amplitude of the initial pulse $U(0,t) = \eta\,\mathrm{sech}(\eta t)$ as a function of the propagation distance for $\delta = 0.5$, $\beta = 10^{-2}$, and $\gamma = 5 \times 10^{-4}$: $\eta = 1$ (solid line), $\eta = 2$ (dashed line), $\eta = 4$ (dashed-dotted), $\eta = 8$ (short dashed-dotted), and $\eta = 14$ (dotted line). (b) Distance of appearance of the stationary soliton x_{EP} (solid line), second pulse (dashed line), and third pulse (short dashed line), as functions of the initial peak amplitude η_N.

TABLE I. Values of parameters, numerical and analytical values of pulse parameters η_N, k_N and η_{PT}, k_{PT}, respectively, as well as the corresponding errors.

$\delta \times 10$	$\beta \times 10^2$	$\gamma \times 10^4$	η_{PT}	k_{PT}	η_N	k_N	$\Delta\eta$	Δk
4.5	2	1	21.007	−8.826	20.963	−8.831	0.21	0.06
4	0.8	50	5.074	−6.436	5.089	−6.426	0.29	0.16
5	0.5	5	12.910	−6.667	12.870	−6.662	0.31	0.07
5	0.75	5	12.297	−4.033	12.283	−4.034	0.12	0.04
5	0.875	5	11.853	−3.211	11.838	−3.217	0.12	0.04
5	1	5	11.392	−2.596	11.385	−2.596	0.06	0.01
5	1.125	5	10.943	−2.129	10.931	−2.129	0.11	0.03
5	1.25	5	10.517	−1.770	10.513	−1.771	0.04	0.08

of p were obtained: $p = 2.354$ [Fig. 3(a)] and $p = 0.549$ [Fig. 3(b)], respectively.

Excellent performance of PT in the description of amplitude evolution should be mentioned. Due to the difference in p the x_{EP} in the second case is much larger. To more precisely check the results obtained by PT, the numerical and analytical values of pulse parameters η_N, k_N and η_{PT}, k_{PT}, respectively, as well as corresponding errors are presented in Table I (first two rows), and excellent agreement between them is identified.

The third aim is to show the suppression of the SSFS for fundamental solitons with large amplitudes $\eta \sim 10$. We fixed the values of $\delta = 0.5$, $\gamma = 5 \times 10^{-4}$, and increased the values of β. The obtained results are also presented in Table I (last six rows).

As can be seen from the last six rows of Table I, with the increase of β, $|k_N|$ reduces, so the suppression of SSFS for the fundamental solitons with large amplitudes ($\eta \sim 13$) is also confirmed. In all cases, starting with initial condition $U(0,t) = \mathrm{sech}(t)$, the distance x_{EP} is very small, $x_{EP} \approx 3$. The excellent agreement (smaller than 1%) between analytical and numerical values of pulse parameters was found. To better study the dependence of the pulse amplitude evolution on the initial conditions $U(0,t) = \eta\,\mathrm{sech}(\eta t)$, where $\eta \subset (1,14)$ for $\delta = 0.5$, $\beta = 10^{-2}$, and $\gamma = 5 \times 10^{-4}$ was calculated through numerical solution of Eq. (1) and the results are presented in Fig. 5(a). Figure 5(b) shows x_{EP} as a function of η_N.

As Fig. 5(a) shows, in all cases the initial pulse transforms into the soliton pulse with the predicted amplitude $\eta_{PT} = 11.39$. The numerical and predicted values for the frequency practically coincide. The additional pulses aroused from the dispersive wave due to the background instability, do not influence the amplitude of the initial pulse (except the small fluctuations) that reaches the equilibrium parameters in all cases. From Fig. 5(b) it can be seen that the increase of the initial amplitude leads to the reduction of x_{EP}. Simultaneously to the process of the formation of the equilibrium soliton, the dispersive waves amplify and the additional pulses appear [33]. Figure 5(b) shows that the distance of appearance of the second and third pulses increases monotonically with η. It was numerically observed that after some propagation distance the second and third pulses achieve the equilibrium parameters.

Finally, we studied the applicability of the analytical descriptions of the change of shape of the pulses in the presence of IRS and BLA. To observe the typical asymmetric changes in the form of the pulses, however, artificially large values of γ should be used. Figure 6(a) compares the results of numerical solution of Eq. (1) (initial condition—soliton, $\eta = a_0 = 1$) with analytical findings [Eqs. (3.5)–(3.6) of [18] and Eq. (10) for $\delta = 5 \times 10^{-2}$, $\beta = 0.4$, and $\gamma = 0.8$]. Figure 6(b) shows the evolution of errors $\varepsilon_{PT,LP} = (\sum_{i=1}^{N} ||U_i^{num}|^2 - |U_i^{PT,LP}|^2|)/\max(|U_i^{num}|^2)$, where N is the number of grid points, U_i^{num} is the numerical values, while U_i^{PT}

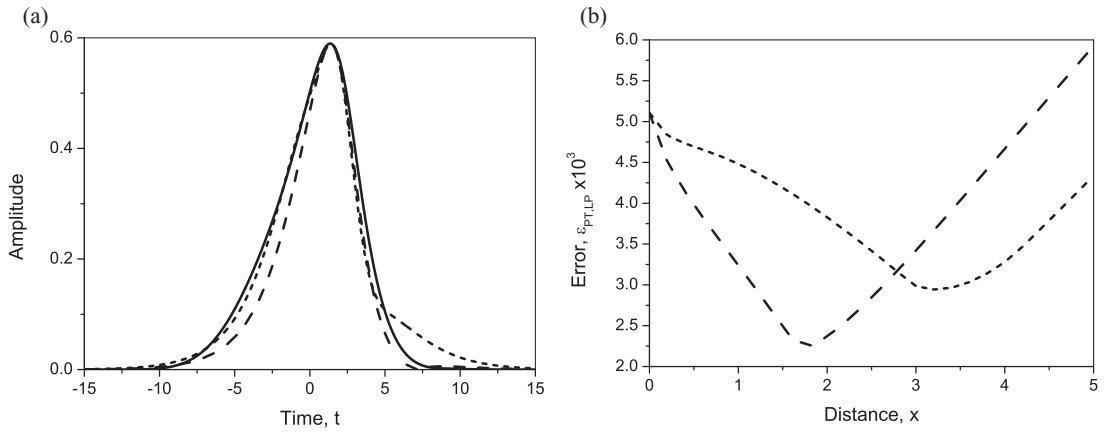

FIG. 6. (a) Comparison between the numerical (solid line) shape and the analytical results of Eqs. (3.5) and (3.6) of [18] (short dashed line) and Eq. (10) (dashed line) of the pulse for $\delta = 5 \times 10^{-2}$, $\beta = 0.4$, $\gamma = 0.8$, and $x = 5$. (b) Evolution of error with distance for (a) Eqs. (3.5) and (3.6) of [18] (short dashed line) and (b) Eq. (10) (dashed line) for $\delta = 5 \times 10^{-2}$, $\beta = 0.4$, and $\gamma = 0.8$.

and U_i^{LP} are the values of solutions given by Eqs. (3.5)–(3.6) of [18] and Eq. (10), respectively.

Figure 6(a) shows that for small values of β both analytical results Eqs. (3.5) and (3.6) of [18] and Eq. (10) describe the numerical results qualitatively well. However, increasing the distance, the error for Eqs. (3.5) and (3.6) of [18] $\varepsilon_{\mathrm{PT}}$ becomes smaller than $\varepsilon_{\mathrm{LP}}$ at $x = 5$: $\varepsilon_{\mathrm{PT}} = 4.34 \times 10^{-3}$, while $\varepsilon_{\mathrm{LP}} = 5.93 \times 10^{-3}$ [Fig. 6(b)]. The values of errors show that earlier derived analytical expressions well describe the numerical findings (at least at the distances considered). The values of errors compare well with those of [40].

IV. CONCLUSION

We numerically analyzed the suppression of the SSFS as well as the compression of short pulses in the presence of BLA (the parabolic approximation). The process of amplification and compression of the initial soliton includes simultaneous generation and amplification of the dispersive waves due to the background instability as well as the formation of new additional solitons [33]. The applicability of the information provided by the EP derived by the PT [31,33–35] has been investigated. Analyzing the equilibrium amplitudes as a function of physical parameters, the maximum compression factor in the amplification of short pulses is revealed. The eigenvalues of the linearized problem in the vicinity of EP [35] allowed determination of the type of equilibrium points as well as estimation of the necessary distance of propagation for the appearance of equilibrium states from different initial conditions. Stationary pulses that correspond to the stable focal points with large amplitudes have been found from different initial conditions, which appear at typical distances of several dispersion lengths. This result presents an analytical understanding for the final stage of amplified and compressed short pulses in the presence of IRS and can have practical applications for the generation of short optical solitons. The relation between the equilibrium amplitude and the speed of the perturbed soliton [see Eqs. (5) and (9)] found analytically earlier in [31,33–35] was numerically proven. Independently of the complicated process of amplification and compression of the initial soliton, all results obtained by PT were confirmed with excellent accuracy by means of direct numerical solution of the basic equation (1). Due to the background instability however, obtained perturbation results have a limited area of application that can be estimated through numerical solution of the basic equation. Finally, it has been shown that the numerically calculated changes in the shape of the perturbed soliton in the presence of BLA and IRS correspond well to the analytical results of [10,18,19] as well as compare qualitatively well to those of [35].

ACKNOWLEDGMENTS

This research was supported by the Project 102 ни 122 – 20 with the Technical University-Sofia, Bulgaria.

[1] A. Hasegawa and Y. Kodama, *Solitons in Optical Communications* (Clarendon, Oxford, 1995).
[2] G. P. Agrawal, *Nonlinear Fiber Optics*, 3rd. ed. (Academic, New York, 2001).
[3] G. P. Agrawal, *Applications of Nonlinear Fiber Optics* (Academic, New York, 2001).
[4] N. N. Akhmediev and A. Ankiewicz, *Solitons: Nonlinear Pulses and Beams* (Chapman and Hall, London, 1997).
[5] J. R. Taylor, *Optical Solitons —Theory and Experiment* (Cambridge University Press, Cambridge, 1992).
[6] L. F. Molenauer and J. P. Gordon, *Solitons in Optical Fibers* (Academic, Boston, 2006).
[7] E. M. Dianov, A.Ya. Karasik, P. V. Mamyshev, A. M. Prokhorov, V. N. Serkin, M. F. Stelmakh, and A. A. Fomichev, JETP Lett. **41**, 294 (1985).
[8] F. M. Mitschke and L. F. Mollenauer, Opt. Lett. **11**, 659 (1986).
[9] V. N. Serkin, Sov. Tech. Phys. Lett. **13**, 320 (1987).
[10] Y. Kodama and A. Hasegawa, IEEE J. Quantum Electron. **23**, 510 (1987).
[11] K. Tai, A. Hasegawa, and N. Bekki, Opt. Lett. **13**, 392 (1988).
[12] M. Gölles, I. M. Uzunov, and F. Lederer, Phys. Lett. A **231**, 195 (1997).
[13] M. Kolesik, L. Tartara, and J. V. Moloney, Phys. Rev. A **82**, 045802 (2010).
[14] R. V. Raja, K. Porsezian, and K. Nithyanandan, Phys. Rev. A **82**, 013825 (2010).
[15] N. Vukovic and N. G. R. Broderick, Phys. Rev. A **82**, 043840 (2010).
[16] J. P. Gordon, Opt. Lett. **11**, 662 (1986).
[17] I. M. Uzunov and V. S. Gerdjikov, Phys. Rev. A **47**, 1582 (1993).
[18] L. Gagnon and P. A. Belanger, Phys. Rev. A **43**, 6187 (1991).
[19] L. Gagnon and P. A. Belanger, Opt. Lett. **15**, 466 (1990).
[20] I. M. Uzunov and V. I. Pulov, Phys. Lett. A **372**, 2730 (2008).
[21] V. N. Serkin, T. L. Belyaeva, G. H. Corro, and M. Agiiero Granados, Quanum Electron. **33**, 456 (2003).
[22] T. L. Belyaeva, V. N. Serkin, C. Hernandez-Tenorio, and F. Garcia-Santibanez, J. Mod. Opt. **57**, 1087 (2010).
[23] V. N. Serkin, A. Hasegawa, and T. L. Belyaeva, Phys. Rev. Lett. **98**, 074102 (2007).
[24] H. H. Chen and C. S. Liu, Phys. Rev. Lett. **37**, 693 (1976).
[25] M. Nakazawa, H. Kubota, K. Kurokawa, and E. Yamada, J. Opt. Soc. Am. B **8**, 1811 (1991).
[26] J. K. Lucek and K. J. Blow, Phys. Rev. A **45**, 6666 (1992).
[27] V. N. Serkin and V. A. Vysloukh, in *Nonlinear Guided Wave Phenomena*, Technical Digest Vol. 15 (Optical Society of America, Washington DC, 1993), Paper No. TuB14, p. 236.
[28] V. N. Serkin, V. A. Vysloukh, and J. R. Taylor, Electron. Lett. **29**, 12 (1993).
[29] V. A. Vysloukh, V. N. Serkin, A. Yu. Danileiko, and E. V. Samarina, Quantum Electron. **25**, 1095 (1995).
[30] G. P. Agrawal, Phys. Rev. A **44**, 7493 (1991).
[31] K. J. Blow, N. J. Doran, and D. Wood, J. Opt. Soc. Am. B **5**, 1301 (1988).
[32] M. Nakazawa, K. Kurokawa, H. Kubota, and E. Yamada, Phys. Rev. Lett. **65**, 1881 (1990).

[33] V. V. Afanasiev, V. N. Serkin, and V. A. Vysloukh, Sov. Lightwave Commun. **2**, 35 (1992).
[34] M. F. S. Ferreira, Opt. Commun. **107**, 365 (1994).
[35] I. M. Uzunov, Phys. Rev. E **82**, 066603 (2010).
[36] Y. Y. Chen and S. H Chen, Nonlinear Dyn. **58**, 417 (2009).
[37] Y. Y. Chen, S. H. Chen, and K. Y. Sze, Acta Mech. Sin. **25**, 721 (2009).
[38] K. Blow and D. Wood, IEEE J. Quantum Electron. **25**, 2665 (1989).
[39] V. N. Serkin, T. L. Belyaeva, G. H. Corro, and M. Agiiero Granados, Quantum Electron. **33**, 325 (2003).
[40] J. Hult, J. Lightwave Technol. **25**, 3770 (2007).
[41] Y. Kodama and A. Hasegawa, Opt. Lett. **17**, 31 (1992).
[42] A. Mecozzi, D. Moores, H. A. Haus, and Y. Lai, Opt. Lett. **16**, 1841 (1991).